Reducing Total Annualized Cost and CO_2 Emissions in Batch Distillation: Dynamics and Control

Gara Uday Bhaskar Babu and Amiya K. Jana
Energy and Process Engineering Laboratory, Dept. of Chemical Engineering, Indian Institute of Technology, Kharagpur 721 302, India

DOI 10.1002/aic.14076
Published online March 17, 2013 in Wiley Online Library (wileyonlinelibrary.com)

In this contribution, the direct vapor recompression approach is introduced in a batch distillation operated at an unsteady state condition. This vapor recompressed batch distillation (VRBD) accompanies an isentropic compressor that runs at a fixed as well as variable speed. Aiming to ensure the optimal use of internal heat source, an open-loop control policy is proposed for the VRBD that adjusts either the overhead vapor splitting or the external heat supply to the reboiler. Again, the variable speed VRBD additionally involves the manipulation of compression ratio. Developing two alternative configurations of VRBD column, the best heat integrated scheme is attempted to identify in the aspects of energy efficiency and total annualized cost for further advancement. A closed-loop control algorithm for the best performing variable speed VRBD aiming to meet the end objective of relatively high-purity product discharged at a constant composition is developed. The separation of a reactive system is considered to illustrate these results and demonstrate the effectiveness of the novel VRBD scheme. Performing simulation tests, it is investigated that the closed-loop control operation substantially improves not only the distillate purity but also the total amount of product. Achieving significant improvement in thermodynamic efficiency and cost by the controlled heat integrated scheme over its conventional counterpart, finally the attractiveness of the VRBD column by investigating its potential to reduce the greenhouse gas (i.e., CO_2) emissions is shown. © 2013 American Institute of Chemical Engineers *AIChE J*, 59: 2821–2832, 2013

Keywords: vapor recompression, variable speed compressor, open-loop control, closed-loop control, reactive batch distillation, energy savings, CO_2 emissions, economics

Introduction

Since 1978, rising surface temperature and greenhouse gas concentrations observed are particularly noteworthy. In fact, 9 of the 10 warmest years on record have occurred during the past decade.[1] Studies show that the carbon dioxide (CO_2) alone is responsible for about two-thirds of the enhanced greenhouse effect.[2,3] A major contribution to this greenhouse gas (i.e., CO_2) emitted to the atmosphere is attributed to fossil fuel combustion, which accounts for almost 98% of total CO_2 emissions in the US for the year 1999[4] and 95% of that in the UK for the year 2000.[5] To meet the environmental targets as agreed in the Kyoto Protocol, it is an absolute necessity to reduce the greenhouse gas emissions (e.g., CO_2).

Distillation is the most mature and extensively used separation process in the chemical and process industries. In the US, about 10% of the industrial energy consumption accounts for distillation alone.[6] Unfortunately, the overall thermodynamic efficiency of a conventional distillation is around 5–20%.[7] Renewed interest in enhancing energy efficiency of distillation processes has been motivated by several factors. Most notable ones include increasing fossil fuel prices, uncertainty of their long-term availability, emission of climate-changing gases, and national goals to reduce dependence on foreign energy sources.

Various thermally coupled distillation configurations have been scrutinized seeking lower energy consumption and better profitability. For example, the Petlyuk column or divided-wall column[8–12] has been successfully commercialized after several decades of research. Other two popular schemes are based on internal energy integration (e.g., internally heat integrated distillation column (HIDiC))[3,13–19] and external energy integration (e.g., direct vapor recompression column (VRC)).[20–24] By performing operational and economic analysis, a systematic comparison between the HIDiC and VRC is presented in the literature.[25] In particular, the heat pump system has been emerging as an important scheme, because it is easy to introduce and the plant operation is usually simpler compared to other heat integration strategies.[26] However, all these aforementioned schemes are designed and developed for continuous flow distillation columns. Yet studies addressing the thermal integration of batch distillation are very rarely reported in the literature. It is with this intention that this work has been undertaken.

Batch processing has continued to be an important technology owing to the greater operational flexibility that it offers. This operational flexibility of batch distillation

Correspondence concerning this article should be addressed to A. K. Jana at akjana@che.iitkgp.ernet.in.

processes makes them particularly suitable for smaller, multiproduct, or multipurpose operations. Manufacturing in the pharmaceutical and specialty chemical industries are examples of small, multiproduct operations, where products are typically required in small volumes, and subject to short product cycles and fluctuating demand. The thermodynamic disadvantage of batch distillation over continuous fractionation, which results in lower energy efficiency, has long been known.

Takamatsu et al.[27] are the first to configure a thermally integrated batch distillation scheme, in which, the rectification tower is surrounded by a jacketed reboiler. Maiti et al.[28] have further systematized the idea and clarified the advantages of this internally heat integrated scheme through numerical simulations. Recently, an externally energy intensified batch distillation is devised by researchers[29,30] under the framework of direct VRC mechanism. In their strategy, the VRC system operates in conjunction with a variable speed compressor. It has been revealed that such an integrated configuration leads to significant energy and, thus, cost savings.

This work aims at exploring the feasibility of fixed speed as well as variable speed vapor recompression techniques in a batch distillation. To ensure the effective use of internal heat source, an open-loop control policy is devised for the vapor recompressed batch distillation (VRBD) arrangement. To evaluate the comparative performance of the open-loop VRBD schemes in the aspects of energy efficiency and cost, a reactive batch distillation example is chosen for simulation. Subsequently, the most effective thermally coupled configuration (i.e., variable speed VRBD) is further investigated with a closed-loop control scheme. The principle objective of this closed-loop operation is to obtain relatively high-purity product at a constant composition from the top. Performing several simulation experiments on the representative reactive system, the energetic and economic potentials of the closed-loop variable speed VRC are quantified with reference to its conventional counterpart. The attractiveness of the proposed heat pump system is also measured by its ability in reducing CO_2 emissions. This is probably the first article that investigates the thermodynamic and economic performance of a controlled VRBD.

Conventional Batch Distillation

Process description

The two most common configurations of batch distillation column are the batch rectifier and batch stripper. This study deals with the batch rectifier, and we call this scheme as the conventional batch distillation (CBD), hereafter. As shown in Figure 1, it consists of an overhead condenser and a bottom reboiler (or still pot) above which the rectifying section is mounted. The CBD usually operates in two sequential modes under open-loop operation. Distributing initial charge in the reboiler and condenser, and on the trays, the batch column starts running with a condition of complete reflux recycling to attain the steady state (startup phase). Subsequently, the distillate is sequentially removed from the top of the column under partial reflux mode (production phase). Interestingly, the lightest component withdrawal is sometimes begun, as soon as this component met the composition specification, without waiting for the steady state to be attained. Note that the product withdrawal is continued, until the average distillate composition meets the desired product purity.

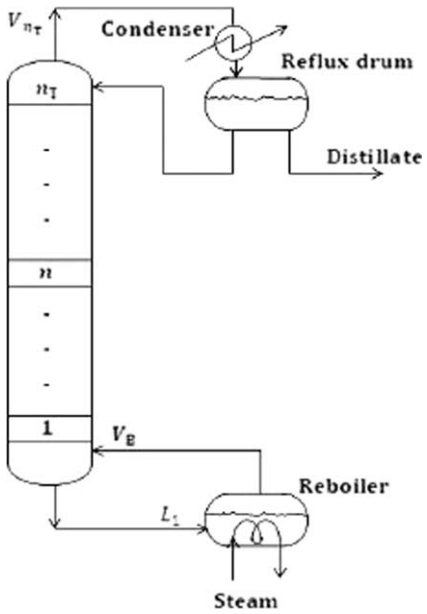

Figure 1. Schematic representation of CBD column.

Mathematical modeling

Most commonly used assumptions in formulating the dynamic model of a CBD include: perfect mixing and equilibrium on all trays, negligible tray vapor holdups and fast energy dynamics. For deriving the modeling equations, let us consider a typical *n*th tray, in which a liquid-phase reaction takes place. As demonstrated in Figure 2, the plate is fed with a liquid feed mixture. Side streams are withdrawn as a liquid as well as a vapor. The material balance, vapor-liquid equilibrium, mole fraction summation and heat balance (MESH) equations are as follows

Total mole balance

$$\dot{m}_n = L_{n+1} + V_{n-1} + F_n - \left(L_n + S_n^{\mathrm{L}}\right) - \left(V_n + S_n^{\mathrm{V}}\right) + R_{\mathrm{f}} \sum_{j=1}^{C} \delta_j r_n \varepsilon_n \tag{1}$$

Component mole balance

$$\dot{m}_n \dot{x}_{n,j} = L_{n+1} x_{n+1,j} + V_{n-1} y_{n-1,j} + F_n z_{n,j} - \left(L_n + S_n^{\mathrm{L}}\right) x_{n,j} - \left(V_n + S_n^{\mathrm{V}}\right) y_{n,j} + R_{\mathrm{f}} \delta_j r_n \varepsilon_n \tag{2}$$

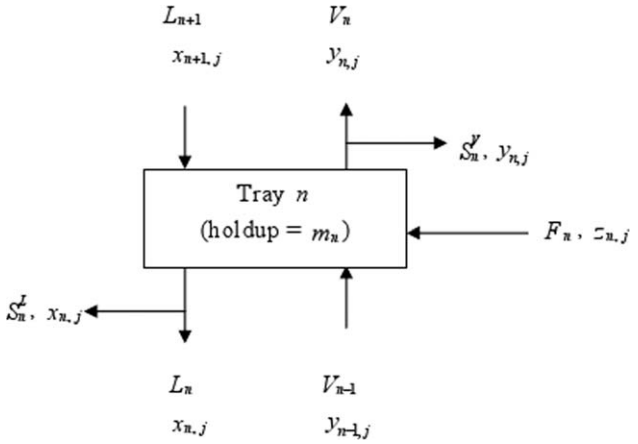

Figure 2. A typical *n*th reactive plate.

Energy balance

$$\dot{m}_n\dot{H}_n^{\mathrm{L}}=L_{n+1}H_{n+1}^{\mathrm{L}}+V_{n-1}H_{n-1}^{\mathrm{V}}+F_nH_n^{\mathrm{F}}-\left(L_n+S_n^{\mathrm{L}}\right)H_n^{\mathrm{L}} -\left(V_n+S_n^{\mathrm{V}}\right)H_n^{\mathrm{V}}+R_{\mathrm{f}}r_nH_n^{\mathrm{r}}\varepsilon_n-Q_n \tag{3}$$

Equilibrium

$$y_{n,j}=k_{n,j}x_{n,j}=\frac{P_{n,j}^0}{P_{\mathrm{T}}}x_{n,j} \tag{4}$$

Summation

$$\sum_{j=1}^{C}x_{n,j}=1 \tag{5a}$$

$$\sum_{j=1}^{C}y_{n,j}=1 \tag{5b}$$

In the aforementioned equations, x denotes the liquid-phase composition, y the vapor-phase composition, z the feed composition, L the liquid flow rate, V the vapor flow rate, k the vapor–liquid equilibrium coefficient, H the enthalpy, H^{r} the heat of reaction, C the total number of components, P_{T} the total pressure, P^0 the vapor pressure, Q the heat loss, F the feed flow rate, S the flow rate of side stream, r the reaction rate, ε the volume of tray liquid, and δ the stoichiometric coefficient. The subscript/superscript n indicates the tray index, j the component index, F the feed, L the liquid stream, and V the vapor stream. Note that R_{f} is a multiplication factor that takes values equal to zero for non-reactive and one for reactive stage.

Heat of formation is considered while computing the enthalpies of streams by means of which the heat of reaction term can be removed from the energy balance equation. Moreover, in the simulation, algebraic form of equations[31] has been used to compute the vapor and liquid enthalpies. It is well known that for a batch distillation, values of feed flow rate (F) and bottom flow rate (B) are taken as zero. Moreover, if there are no side draws, then we consider $S^{\mathrm{L}}=S^{\mathrm{V}}=0$. Negligible heat loss from a stage to the surroundings ($Q_n=0$) is also assumed. Note that it is straightforward to extend this modeling approach to other trays.

VRBD

Principle and configuration

In a conventional distillation process, the top temperature is less than the bottom one. The heat is added at the highest temperature point in the column (i.e., reboiler), and it is rejected at the lowest temperature point (i.e., condenser), leading to the degradation of heat from a higher temperature level to a lower temperature level. To improve the thermodynamic efficiency, the rejected heat must be reutilized, so that the supply of thermal energy from an external source can get reduced. An obvious way to achieve this goal is to couple the condenser and the reboiler which represent the major source and sink of energy, respectively.

We know that the heat flows naturally from a higher to a lower temperature. Heat pumps, however, are capable of forcing the heat flow in the reverse direction using a relatively small amount of high-quality drive energy (e.g., electricity). Hence to reuse the heat rejected in the condenser of a distillation column, its temperature should be raised by some form of heat pump.

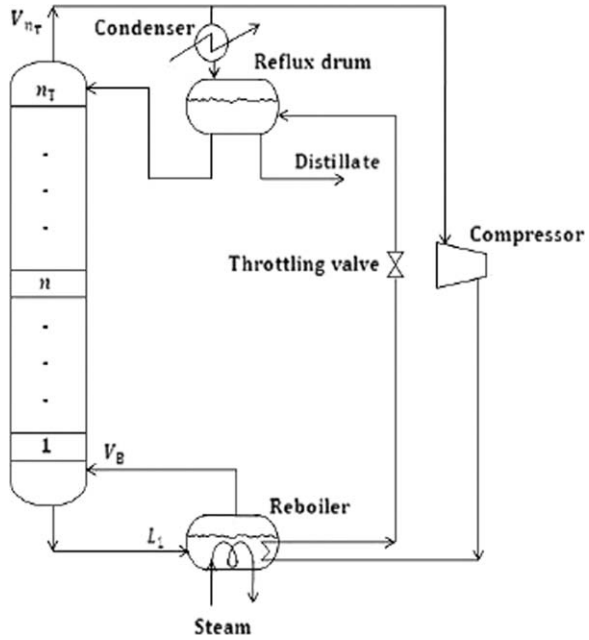

Figure 3. Schematic representation of VRBD column.

The concept of using heat pumps in continuous distillation has been known for a long time.[32] Among its various forms, the direct VRC is the simplest and effective application of heat pumps in distillation.[18] In this article, we select the VRC scheme for batch processing.

Figure 3 schematically demonstrates the principles of VRBD column. In this arrangement, vapor from the top of the batch column is compressed to the desired pressure (hot stream) and condensed against reboiler liquid (cold stream). This in turn boils the reboiler content, generating vapor that enters the rectifying tower. Although the overhead stream changes its phase to liquid state, it leaves the still at elevated pressure. Before its entry into the reflux drum, the condensate is depressurized by a pressure relieve valve. By this way, the proposed heat integration creates an opportunity for recovering heat from the top vapor and, thus, reduces the hot utility requirements. In addition, this scheme leads to the reduction of operating and equipment costs of the overhead condenser. However, the VRBD column additionally involves a compressor, and it requires electrical energy, which is much more expensive than the thermal utility. Therefore, it is indeed not so straightforward to comment that the VRBD has the potential to save energy compared to the conventional stand alone column. Thus, in this study, we aim to conduct a quantitative analysis.

Dynamic model

The vapor recompression arrangement mainly consists of an isentropic compressor and a throttling valve. Therefore, the dynamic model of VRBD includes the all modeling equations of CBD column in addition to the equations representing the pressure changers. For the heat integrated scheme, it is supposed that there is no superheating occurred in the compressor as well as no flashing in the valve. The compressor duty, Q_{Comp} (in hp) is computed as[33]

$$Q_{\mathrm{Comp}}=3.03\times10^{-5}\frac{\mu}{\mu-1}V_{\mathrm{T}}P_{\mathrm{i}}\left[\left(\frac{P_{\mathrm{C}}}{P_{\mathrm{i}}}\right)^{\frac{\mu-1}{\mu}}-1\right] \tag{6}$$

In this equation, the pressure (inlet pressure, P_i and outlet pressure, P_C) is in lb_f/ft^2, and the vapor inflow rate to the compressor (V_T) is in ft^3/min. The polytropic coefficient of species j (μ_j) is temperature dependent, and the value of μ is calculated from

$$\frac{1}{\mu-1}=\sum_{j=1}^{C}\frac{y_j}{\mu_j-1} \tag{7}$$

Open-loop control policy

To ensure the optimal use of internal heat source under the VRC framework, in this section, an open-loop control algorithm is devised. This control strategy is synthesized with classifying the VRBD into two schemes, namely, the fixed speed VRBD and the variable speed VRBD, and both of these schemes are presented later.

To perform a meaningful comparison between the VRBD and its conventional analogous, this work attempts to keep the input conditions (e.g., feed charge and composition and reboiler duty) and output specifications (e.g., product purity and amount) same. Among them, the reboiler heat input (Q_R), which is maintained constant throughout the entire batch processing, plays a crucial role in thermal coupling because of the transient behavior of batch operation. Obviously, the other input and output conditions can easily be kept unaltered between the CBD and VRBD columns.

Prior to controller synthesis, we assume that the compressed overhead vapor (at T_{TC}) completely condenses in the reboiler (at T_B), if there exists a temperature driving force, ΔT_C ($=T_{TC}-T_B$) of at least 20°C. Accordingly, we select the two operating criteria for the VRBD as: (1) $\Delta T_C \geq 20°C$ and (2) constant Q_R. To meet these objectives, now we aim to formulate an open-loop control policy with a suitable variable manipulation mechanism.

Operating Criterion 1 ($\Delta T_C \geq 20°C$). Based on our assumption stated earlier, we can operate the heat integrated scheme with a bounded $\Delta T_C (\geq 20°C)$ to ensure the phase change of entire vapor. To serve the same purpose, the column can also be operated with an exact ΔT_C of 20°C. Accordingly, we classify the VRBD operation into two modes as: fixed speed VRBD ($\Delta T_C \geq 20°C$) and variable speed VRBD ($\Delta T_C = 20°C$). Both of these configurations include a heat pump for overhead vapor recompression. In the former scheme, the compressor runs at a fixed compression ratio (CR), whereas in the later scheme, the compressor operates at a variable speed, and, therefore, they are called so. We come now to discuss how the operating criterion concerning ΔT_C is satisfied in these two modes of operation.

Fixed speed VRBD. To formulate the operating policy for the VRBD that should run at a fixed speed (i.e., at a fixed CR) with satisfying the criterion mentioned earlier, we first need to detect the time instant at which the ΔT_T ($=T_B-T_T$) is maximum. Here, T_T denotes the top vapor temperature. Actually, the highest ΔT_T corresponds to the maximum CR requirement, and the implementation of this CR can only ensure the batch operation with $\Delta T_C \geq 20°C$.

The following expression can be used for calculating the CR

$$\mathrm{CR}=\frac{P_C}{P_i}=\left(\frac{T_{TC}}{T_T}\right)^{\mu/(\mu-1)} \tag{8}$$

Here, $T_{TC}=T_B+20°C$. Recall that P_i and P_C represent the inlet and outlet pressure of top vapor, respectively, with respect to the compressor.

Variable speed VRBD. In this configuration, an attempt is made to run the column with an exact ΔT_C of 20°C aiming to avoid the compressor operation at a maximum CR throughout the whole batch operation. Accordingly, the CR would vary at every time step because of the variation of both reboiler and top vapor temperatures. The same expression (i.e., Eq. 8) is used to manipulate the CR dynamically.

Operating Criterion 2 (Constant Q_R). This operating criterion is applicable to both the fixed speed and the variable speed VRBD column. Thus, there is no involvement of separate manipulation policies to fulfill the second criterion.

In the VRBD scheme, the compressed vapor releases heat (Q_{CV}), which in turn leads to the reduction of external heat input to the still (Q_E). It implies

$$Q_R=Q_{CV}+Q_E \tag{9}$$

Because of the unsteady state characteristics of batch column, the Q_{CV} should vary with time. Under this circumstance, there are two possibilities arise as: $Q_{CV} > Q_R$ (Scenario 1) and $Q_{CV} < Q_R$ (Scenario 2). Now, we develop the control scheme for these two scenarios.

Scenario 1 ($Q_{CV} > Q_R$). In this case, the latent heat (λ) released by the top vapor in the still is more than the heat required for liquid reboiling. It is experienced that the use of this extra heat (i.e., $Q_{CV}-Q_R$) does not necessarily improve the batch processing, particularly when the setup is run with optimal Q_R. Rather, it delays the startup operation because of the reboiling of relatively heavier fraction by that extra heat. This fact clearly demonstrates the necessity of overhead vapor (V_T) splitting, so that a fraction of it (V_{TC}) can exactly alter the heat required by the still pot (i.e., Q_R) and the rest amount (V_{Ti}) can be directed to the overhead condenser. For this, the V_{TC} can be calculated as

$$V_{TC}=\frac{Q_R}{\lambda\ (\text{at } T_{TC})} \tag{10}$$

Now, one can easily obtain the V_{Ti} by subtracting V_{TC} from V_T. It becomes clear that when $Q_{CV} > Q_R$, the VRBD requires to manipulate the overhead vapor splitting.

Scenario 2 ($Q_{CV} < Q_R$). In this scheme, the heat available from internal source is not adequate to run the column with the same dynamical features. Therefore, the balance of the heat requirements of the column (i.e., Q_R-Q_{CV}) is supplied by steam (an external heating medium) to the still. Obviously, in this case, the VRBD involves the manipulation of steam flow rate (m_S)

$$m_S\lambda_S=Q_E=Q_R-Q_{CV} \tag{11}$$

where the λ_S represents the latent heat of steam.

It is worth noticing that this open-loop control law is formulated to compute a single manipulated variable for the fixed speed VRBD, that is, either the vapor inflow rate to the compressor, V_{TC} (when $Q_{CV} > Q_R$) or the auxiliary heat input to the still from an external source, Q_E (or m_S) (when $Q_{CV} < Q_R$). On the other hand, the variable speed scheme simultaneously adjusts the CR along with either the V_{TC} or the Q_E.

Quantitative Performance Analysis

To demonstrate the potential of the proposed VRBD column, a quantitative analysis is performed in terms of several

indexes, namely, the thermal efficiency, greenhouse gas emissions, and total annualized cost (TAC).

Thermal efficiency

Knowing the reboiler duty, it is indeed quite straightforward to estimate the total heat consumed by a CBD ($Q_{\text{Cons}}^{\text{CBD}}$) throughout the entire batch operation. However, in case of VRBD structure, it gets a bit complicated. In the heat integrated scheme, there are two sources of thermal energy used: one is the internal source that provides heat through overhead vapor condensation (Q_{CV}) and other one is the steam that is supplied externally (Q_{E}). As stated previously, before thermally coupling the whole amount of top vapor or a fraction of it, a compressor has to be installed, and it involves an additional energy component as compressor duty (Q_{Comp}).

As suggested by Iwakabe et al.,[34] it is logical to assume that 3 kW of thermal energy is needed to produce 1 kW of electrical power. Accordingly, the total heat consumption in a VRBD ($Q_{\text{Cons}}^{\text{VRBD}}$) is estimated as

$$Q_{\text{Cons}}^{\text{VRBD}} = Q_{\text{E}} + 3Q_{\text{Comp}} \tag{12}$$

This correlation is applicable to both the fixed speed and the variable speed scheme. Furthermore, the external heat input gets the following form depending on the availability of Q_{CV} as

$$\begin{cases} Q_{\text{E}} = 0 & \text{for Scenario 1} \\ Q_{\text{E}} = Q_{\text{R}} - Q_{\text{CV}} & \text{for Scenario 2} \end{cases}$$

It should be pointed out that for CBD column

$$\begin{cases} Q_{\text{E}} = Q_{\text{R}} \\ Q_{\text{Comp}} = 0 \end{cases}$$

Calculating the $Q_{\text{Cons}}^{\text{CBD}}$ and $Q_{\text{Cons}}^{\text{VRBD}}$ based on the concept detailed earlier, one can readily find the percent savings in thermodynamic efficiency.

Model for CO_2 emissions

Carbon dioxide as a greenhouse gas plays a crucial role in global warming. It is reported[2,3] that the two-thirds of the enhanced greenhouse effect are caused by CO_2 alone. In this contribution, we estimate the greenhouse gas emissions (i.e., CO_2) from the combustion processes associated with the utility systems. It is a fact that compared to the original processes (e.g., distillation column), the concerned utility systems usually generate much larger volume of greenhouse gases.[35]

In the CBD column, we use steam for liquid reboiling, while the heat integrated scheme requires steam for the same purpose and power (electricity) to drive the compressor. Therefore, the two utility systems, steam boiler and gas turbine, are selected to use for the generation of steam and power, respectively. In energy savings oriented projects and reducing environmental emissions impacts, these utility devices are the key drivers.

In this work, we compare the emission levels using natural gas and low sulfur diesel as heating fuels in both the utility devises. In the utility system, CO_2 emissions are related to the amount of fuel burnt by the following stoichiometric equation as[3,35]

$$\text{C}_n\text{H}_m + \left(n + \frac{m}{4}\right)\text{O}_2 \rightarrow n\text{CO}_2 + \frac{m}{2}\text{H}_2\text{O} \tag{13}$$

Air must be supplied to burners in excess to ensure complete combustion. It is true that the amount of CO can be reduced to negligible levels by excess supply of air, proper burner design, regular maintenance, and adequate control. Here, we assume that all carbon in the fuel is reacted to CO_2.

In a heating devise, CO_2 emissions are related as

$$\text{CO}_2 \text{ flow rate } (\text{kg/h}) = \frac{Q_{\text{Fuel}}}{\text{NHV}} \times \frac{\text{C\%}}{100} \times \alpha \tag{14}$$

where Q_{Fuel} represents the heat duty from fuel burnt (kJ/h), fuel net heating value (NHV) the fuel net heating value (kJ/kg), C% the mass percentage carbon in fuel, and α the ratio of CO_2 and carbon molar masses (=3.67). Data for heating fuels are taken from Smith and Delaby[35] and documented in Table 1.

CO_2 Emissions from Steam Boiler. The fuel is combusted when mixed with air, producing flue gases that can be used as a heat source in the utility systems. Actually, the flue gases release heat when they are cooled from the flame temperature (T_{FT}) to the stack temperature (T_{Stack}). For a steam boiler, the flame temperature (T_{FTB}) and T_{Stack} are adopted as 1800°C and 160°C, respectively.[35]

The steam may be produced in a steam boiler either at the temperature required by the process or at a higher temperature and then throttled. In the later scheme, the boiler feed water (FW) is added after expansion (desuperheating) to maintain the steam quality.

Making a heat balance around the boiler, we obtain

$$Q_{\text{Fuel}} = \frac{Q_{\text{Proc}}}{\lambda_{\text{Proc}}}(h_{\text{Proc}} - h_{\text{FW}})\frac{T_{\text{FTB}} - T_0}{T_{\text{FTB}} - T_{\text{Stack}}} \tag{15}$$

where λ_{Proc} and h_{Proc} denote the latent heat (kJ/kg) and enthalpy (kJ/kg) of steam delivered to the process, respectively, Q_{Proc} the process heat duty (kW), h_{FW} the enthalpy (kJ/kg) of FW and T_0 the ambient temperature (=25°C). Now, using Eq. 14, one can calculate the CO_2 emissions from steam boiler.

CO_2 Emissions from Gas Turbine. This section deals with the model for combustion of a fuel in a gas turbine. This utility system can typically provide both heat and power to the process. However, here we use it to generate power for the compressor unit integrated in the heat integrated scheme.

The amount of fuel burnt to supply Q_{Proc} can be calculated from

$$Q_{\text{Fuel}} = \frac{Q_{\text{Proc}}}{\eta_{\text{GT}}}\frac{1}{1 - \eta_{\text{C}}} \tag{16}$$

where the efficiency of gas turbine

$$\eta_{\text{GT}} = \frac{T_{\text{out}} - T_{\text{Stack}}}{T_{\text{out}} - T_0} \tag{17}$$

Table 1. Data for Heating Fuels

Fuel	NHV (kJ/kg)	C%
Natural gas	5.16×10^4	75.38
Low sulfur diesel fuel	4.2×10^4	86.2

and the Carnot factor

$$\eta_C = \frac{T_{in} - T_{out}}{T_{in} + 273} \tag{18}$$

Here, T_{in} is the inlet temperature to the gas turbine (i.e., after combustion chamber, °C) and T_{out} the outlet temperature from the gas turbine (°C). These two temperatures vary according to the turbine design. As suggested by Smith and Delaby,[35] T_{in} of 1027°C and T_{out} of 720°C are adopted.

The power (electricity) delivered by a gas turbine, W_{GT} (kW) is estimated by applying a typical mechanical efficiency of 90% from

$$W_{GT} = 0.9\ \eta_C\ Q_{Fuel} \tag{19}$$

Now, the emissions of CO_2 can be calculated from Eq. 14.

It is interesting to note that so far we discussed an approach for calculating the "local emissions" from a gas turbine. The power generated from the gas turbine is either consumed in the process itself or exported to other consumers. In both cases, the central power station, which is situated somewhere else, has the possibility of reducing electricity production by the amount generated by the gas turbine. Thus, certain amounts of fuels can be saved at the central power plant, thereby reducing the CO_2 emissions. This, in turn, leads to a saving in the emissions at the central power station. Hence, the central power plant together with the utility system is suggested[35] to be considered as one unit in emission calculations. The corresponding CO_2 emissions are called "global emissions" and expressed as

$$\text{Global emissions} = \text{emissions from process plant} - \text{emissions saved at central power station} \tag{20}$$

Here, we refer the utility system (i.e., gas turbine) as the process plant in Eq. 21. The efficiency of the power plant is assumed to be 30%.[35]

It should be noted that the same fuel is used in both the utility systems and the central power station, when we compare the emission levels between the VRBD and CBD columns.

Economics

When assessing the relative economics of different arrangements, one must take the capital cost of the system into account as well as the operating costs. Here, the economic evaluation is carried out by estimating the TAC, which is the sum of operating cost and annual capital investment. Annual capital investment is assumed to be capital investment divided by a payback period of 3 years. For costing purposes, we consider the stainless steel (SS) as the main material of construction (MOC). The installed cost estimates, based on correlations proposed by Douglas[33] and given in Table 2, are updated using the Marshall and Swift index (M&S = 1569).[36]

For the sake of simplicity, the operating costs are taken to be identical to utility costs for a year with 8000 operating hours. The required utilities are electricity, low pressure (LP) steam and cooling water with unit costs[37] of \$0.1/kW.h, \$13/t, and \$0.03/t, respectively. It should be highlighted that the operating cost of the compressor is calculated as suggested by Douglas[33] based on the bhp (=hp/0.8) and a motor efficiency of 0.6.

Table 2. Cost Estimating Formula and Parameter Value

• *Column shell* (MOC: SS) Installed cost $(\$) = \left(\frac{M\&S}{280}\right)\ 101.9 D_c^{1.066} L_c^{0.802} (c_{in} + c_m c_p)$ where D_c is the column diameter (ft), L_c the column height (ft), $M\&S = 1569$, and the coefficients $c_{in} = 2.18$, $c_m = 3.67$, and $c_p = 1.0$
• *Column tray* (Type: bubble-cap, MOC: SS) Installed cost $(\$) = \left(\frac{M\&S}{280}\right) 4.7 D_c^{1.55} L_c (c_s + c_t + c_m)$ where the coefficients $c_s = 1$, $c_t = 1.8$, and $c_m = 1.7$
• *Heat exchanger* (MOC: SS) Installed cost $(\$) = \left(\frac{M\&S}{280}\right) 101.3 A^{0.65} \left(c_{in} + c_m \left(c_t + c_p\right)\right)$ where A is the heat transfer area (ft^2), and the coefficients $c_{in} = 2.29$, $c_m = 3.75$, $c_t = 1.35$, and $c_p = 0$
• *Compressor* Installed cost $(\$) = \left(\frac{M\&S}{280}\right) 517.5 (bhp)^{0.82} (2.11 + F_d)$ where $F_d = 1.0$. This expression is valid in the range of $30 < \text{bhp} < 10{,}000$

Closed-Loop Control Algorithm

It is a fact that the batch distillation experiences a great deal of changes from a low-plant-gain composition space (i.e., the steady-state space) to a high-plant-gain composition space.[38] This implies that the controller gain should be increased accordingly during the batch processing. For this, a gain-scheduled proportional integral (GSPI) law is selected for the VRBD process for regulating the distillate composition ($x_{D,i}$) with the manipulation of reflux rate (R).

The constant distillate composition procedure is usually implemented using a feedback control scheme with the manipulation of either reflux flow or distillate flow. The reflux ratio mechanisms are operated in open-loop fashion, that is, predefined values are used without feedback from the process. In this study, we select reflux rate for controlling the distillate composition by the employment of GSPI scheme and distillate rate for maintaining the liquid holdup in reflux accumulator by the use of conventional PI.

The GSPI controller has the following form[39]

$$R = R_S + K_C\left(x_{D,i}\right)\left(e + \frac{1}{\tau_I}\int_0^t e\,dt\right) \tag{21}$$

where $x_{D,i}$ is the scheduling variable. The controller gain, K_C, is varied aiming to keep $K_C K_P$ constant, which then keeps the stability margin unchanged. If the process gain is characterized as a function of the scheduling variable, $K_P\left(x_{D,i}\right)$, then the controller gain can be scheduled as

$$K_C\left(x_{D,i}\right) = \frac{K_C\left(x_{D0,i}\right) K_P\left(x_{D0,i}\right)}{K_P\left(x_{D,i}\right)} \tag{22}$$

The gain of the GSPI scheme has two different forms, depending on the product purity with reference to its desired value, as

1. When $x_{D,i} > x_{D0,i}$,

$$K_C\left(x_{D,i}\right) = K_{C0}\frac{1 - x_{D0,i}}{1 - x_{D,i}} \tag{23}$$

where $K_P\left(x_{D,i}\right) = 1 - x_{D,i}$ and $K_C\left(x_{D0,i}\right) = K_{C0}$.

2. When $x_{D,i} < x_{D0,i}$

$$K_C\left(x_{D,i}\right) = K_{C0} \tag{24}$$

It should be pointed out that this is a "one-way" approach. As the process gain increases with lower purity, maintaining a constant controller gain speeds up the response when the distillate is less pure.

An Illustrative Example: Separation of a Reactive Multicomponent System

Conventional reactive batch distillation

To evaluate the proposed thermally integrated scheme, a reactive batch distillation column example is considered.

We study the esterification of acetic acid with ethanol to produce ethyl acetate.

$$\text{acetic acid} + \text{ethanol} \rightleftarrows \text{ethyl acetate} + \text{water}$$

Boiling point (K)	391.1	351.5	350.3	373.2

The reaction is slightly endothermic and takes place in the liquid phase. The reaction kinetics is reported in Table 3.[40]

The representative column has total eight trays, excluding the reboiler and a total condenser. The trays are counted from bottom to top; bottom tray is the first tray and top tray is the eighth tray. For constructing the dynamic model, the following assumptions have been adopted: negligible tray vapor holdup, variable liquid holdup (except in reflux drum), perfect mixing and equilibrium on all trays, reactions occurred on the trays, and in the condenser and reboiler, fast energy dynamics, no azeotrope formation, constant operating pressure (atmospheric) and tray efficiency (Murphree vapor-phase efficiency = 85%), and Raoult's law for the vapor–liquid equilibrium. The modeling equations for a typical *n*th reactive tray are detailed earlier, and it is indeed quite easy to extend the modeling approach to all other trays.[41] The operating conditions are summarized in Table 3 together with other relevant data about the system.

Simulation Algorithm. The reactive distillation model comprises MESH equations in addition to some algebraic equations representing the tray hydraulics, reaction kinetics, vapor–liquid equilibrium, enthalpy correlations, and so forth. This differential algebraic equation system is simulated with developing a computer code in C/C^{++}. The sequential steps involved in the computer simulation are detailed as follows[41]:

Step 1: Input data on the column size, feed specifications, tray efficiency, reaction information, vapor pressure data, and so forth.

Step 2: *Input data for variables at time t = 0*. The variables include the liquid-phase compositions (x_i) and liquid holdups (m) for all trays.

Table 3. Column Specifications and Reaction Kinetic Data

Column specifications	
System	Acetic acid/ethanol/ ethyl acetate/water
Total feed charge (kmol)	5.0
Feed composition (startup) (mol fract)	0.45/0.45/0.0/0.1
Internal plates holdup (startup) (kmol)	0.1
Reflux drum holdup (kmol)	0.0125
Heat input to the still pot (kJ/min)	1700
Distillate composition (steady state, mol fract)	0.964
Distillate rate (kmol/min)	0.034
Kinetic data	
Rate of reaction (kmol/(L min))	$r = k_1 c_1 c_2 - k_2 c_3 c_4$
Rate constants where c_i = concentration (kmol/L) for the ith component	$k_1 = 4.76\times10^{-4}$; $k_2 = 1.63\times10^{-4}$

Step 3: Either input the values of reflux rate and distillate rate or manipulate these variables using the suitable controllers. Note that in batch operation, the start-up phase runs under total reflux condition (i.e., $D=0$).

Step 4: Compute the equilibrium vapor-phase composition and temperature (T) for each tray based on bubble point algorithm. The Newton–Raphson convergence method is used in the bubble point calculations. Subsequently, calculate the actual vapor-phase composition (y_i) using Murphree relationship.

Step 5: Calculate the liquid- and vapor-phase enthalpies for each tray using the algebraic form of equations.

Step 6: Compute the reaction rate.

Step 7: Calculate the internal liquid flow rates using the Francis-Weir formula and the vapor flow rates solving the energy balance equations.

Step 8: Calculate the liquid holdup on each tray for the future time step ($t+\Delta t$) by solving the total mole balance equation.

Step 9: Compute the liquid-phase compositions on all trays for the future time step ($t+\Delta t$) by solving the component mole balance equations.

Step 10: To continue the process simulation for the next time step, go back to Step 3.

Process Dynamics. Figure 4 depicts the complete profile of batch processing for the representative system. As can be seen from the simulation results that the column achieves a steady-state composition of 96.4 mol % and eventually, the same product purity was obtained by Monroy-Loperena and Alvarez-Ramirez.[42] In the production phase, the batch operation is continued with a fixed distillate rate of 34 mol/min

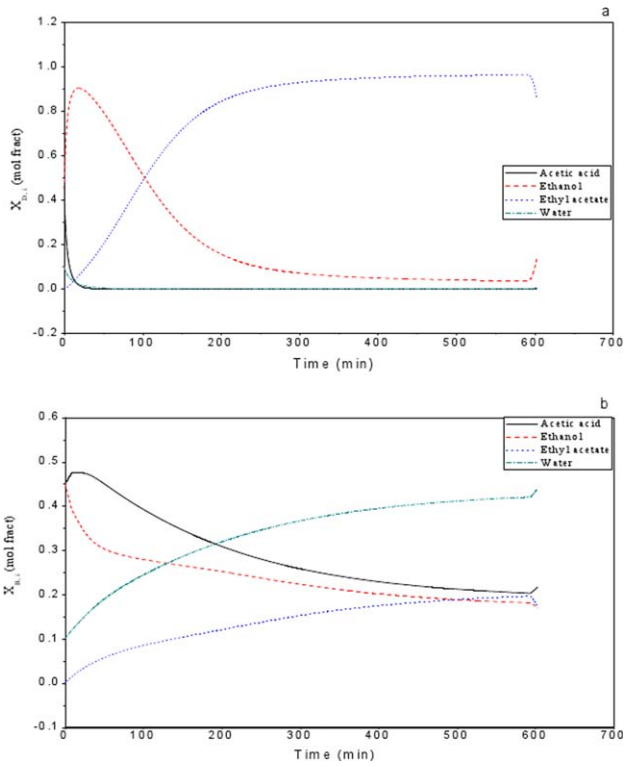

Figure 4. Composition profile throughout the batch operation: (a) reflux drum and (b) reboiler.

[Color figure can be viewed in the online issue, which is available at wileyonlinelibrary.com.]

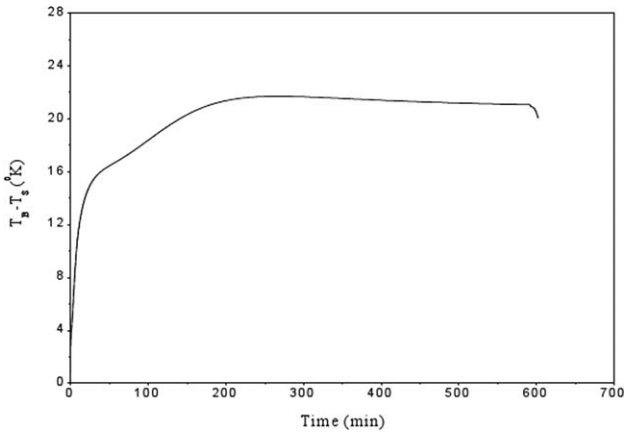

Figure 5. CRBD profile in terms of ΔT_T throughout the batch operation.

(68% of overhead vapor rate, V_8 at steady state) as long as the product composition remains above 86 mol %. Consequently, we get the product purity[1] of 92.83 mol % for a production period of 10.75 min. It is evident in Figure 4 that the startup period (591.82 min) is much larger than the production period, and it is mainly because of selecting a reasonably large product withdrawal rate.

Vapor Recompressed Reactive Batch Distillation Column

Open-loop control policy

The operating principle of VRC mechanism in a batch rectifier is detailed earlier. Applying this mechanism on a reactive batch distillation, we develop a heat integrated structure that is termed as the vapor recompressed reactive batch distillation (VRRBD), hereafter. Recall that the open-loop control law is derived on the basis of two operating criteria concerning ΔT_C and constant Q_R (= 1700 kJ/min). To ensure the condensation of entire compressed vapor, it is attempted to meet the criterion on ΔT_C by developing the two forms of VRRBD column, namely, the fixed speed VRRBD and the variable speed VRRBD. We now synthesize the control strategy for both of these schemes separately.

Fixed Speed VRRBD. The operating procedure of this configuration is formulated by considering (1) $\Delta T_C \geq 20°C$ and (2) $Q_R = 1700$ kJ/min. As stated previously, the CR is fixed to meet the first objective concerning $\Delta T_C \geq 20°C$, and the second criterion on Q_R leads to the manipulation of either the overhead vapor splitting or the external heat input to the reboiler. Accordingly, we first produce the ΔT_T $(=T_B - T_8)$ profile in Figure 5, and it is evident that the maximum ΔT_T exists for a time duration of about 0.51 min (266.83–267.34 min). Using Eq. 8, the CR is calculated as 1.625 with reference to that time duration. Table 4 illustrates the influence of CR and how the CR of 1.625 satisfies the first criterion.

Running the compressor with a fixed CR of 1.625, we also calculate the heat released by the compressed vapor (Q_{CV}) at every time instant. Figure 6 compares the heat available from internal source (i.e., Q_{CV}) with the reboiler

[1]*Average composition of the distillate collected during the entire production period.*

Table 4. Influence of CR on Q_{CV} and ΔT with Reference to the Time Duration of 0.51 min (266.83–267.34 min)

CR	$Q_{CV} \times 10^{-3}$ (kJ/min)	ΔT_C (°C)	CR	$Q_{CV} \times 10^{-3}$ (kJ/min)	ΔT_C (°C)
1	1.659	−21.7	1.625	1.59	20.0
1.5	1.6005	12.8	1.65	1.588	21.4
1.6	1.592	18.6	1.7	1.5842	24.2
1.61	1.5912	19.2	2.0	1.564	39.4
1.62	1.5904	19.8	3.0	1.5184	80.1

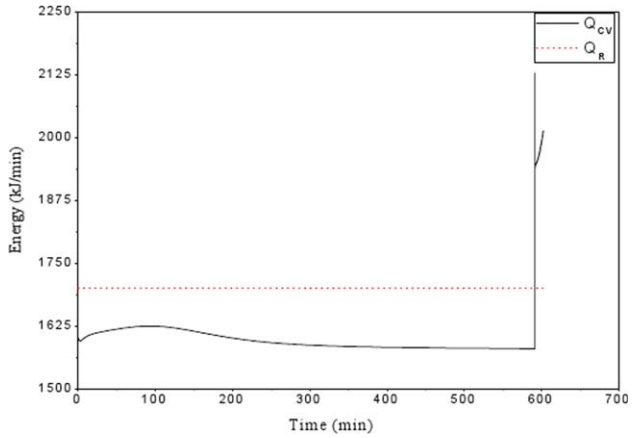

Figure 6. Fixed speed VRRBD profile in terms of Q_{CV} against Q_R.

[Color figure can be viewed in the online issue, which is available at wileyonlinelibrary.com.]

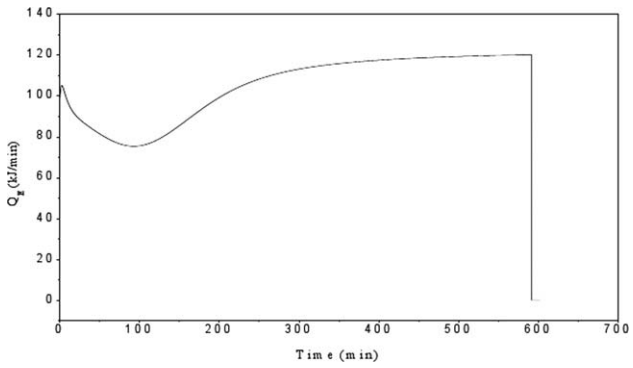

Figure 7. Manipulation profile of Q_E during the startup phase of fixed speed VRRBD.

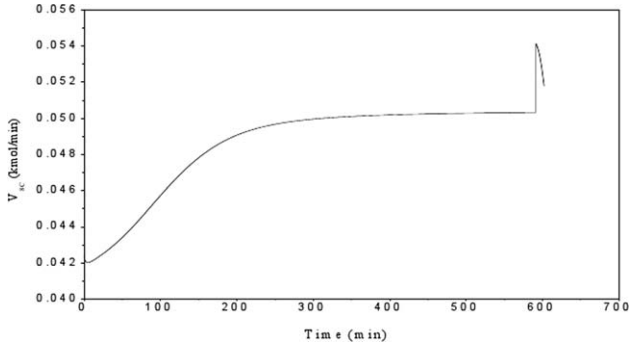

Figure 8. Manipulation profile of V_{8C} during the production phase of fixed speed VRRBD.

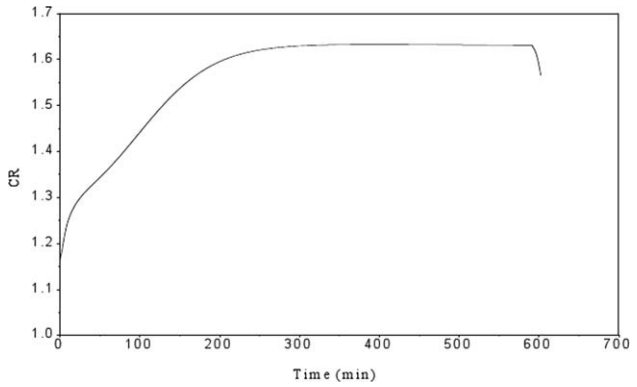

Figure 9. Manipulation profile of CR throughout the operation of variable speed VRRBD.

heat requirements (i.e., Q_R). Analyzing the results, one may readily find that the fixed speed VRRBD falls within the category of Scenario 2 (i.e., $Q_{CV} < Q_R$) during the startup period and Scenario 1 (i.e., $Q_{CV} > Q_R$) during the production period. To operate the column at a constant reboiler load, it is now required to carefully manipulate the auxiliary heat input to the still for the startup phase and the overhead vapor splitting for the production phase. Figures 7 and 8 depict the variable manipulation for the fixed speed VRRBD column under the proposed open-loop control policy.

Variable Speed VRRBD. The variable speed VRRBD configuration differs from the fixed speed VRRBD in the aspect of selecting the first criterion on ΔT_C. Here, it is considered as $\Delta T_C = 20°C$. Accordingly, the CR for the variable speed VRRBD system is determined from Eq. 8 dynamically, and the resulting manipulation profile is displayed in Figure 9.

Comparing Q_{CV} with Q_R in Figure 10, we notice that the variable speed VRRBD, like the fixed speed heat integrated scheme, requires to manipulate both the Q_E and the V_{8C} to validate the second operating criterion of constant Q_R. Figure 11 shows the manipulation of makeup heat, Q_E throughout the startup phase, whereas Figure 12 depicts the adjustment of vapor inflow rate to the compressor, V_{8C} during the production phase.

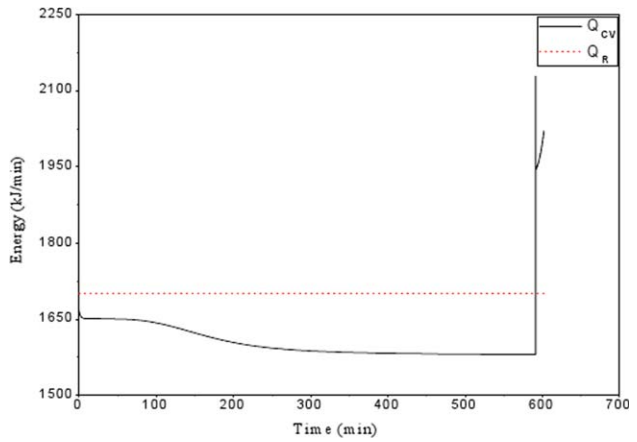

Figure 10. Variable speed VRRBD profile in terms of Q_{CV} against Q_R.

[Color figure can be viewed in the online issue, which is available at wileyonlinelibrary.com.]

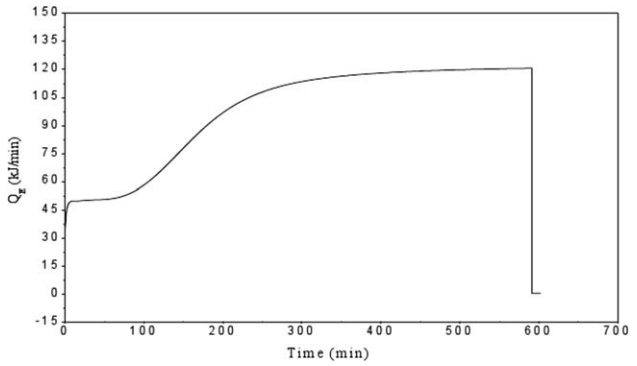

Figure 11. Manipulation profile of Q_E during the startup phase of variable speed VRRBD.

Quantitative Performance Analysis. By applying the open-loop control algorithm, we investigated that both the fixed speed and the variable speed VRRBD columns effectively utilize the internal heat source during the batch operation. It clearly indicates the reduction of utility consumption (i.e., both external heat and cooling medium) and condenser size, leading to an improvement of energetic and economic performance, and CO_2 emission levels.

In this section, the VRRBD column is quantitatively evaluated with reference to the conventional reactive batch column. Here, the conventional reactive batch distillation (CRBD) serves mainly as a baseline for the comparative study. It is observed from simulation results that the heat integration secures a 81.35 and 82.81% energy savings for fixed speed and variable speed VRRBD, respectively. In Table 5, an economic comparison is further made between these schemes. One may readily find that the fixed speed configuration cuts the operating cost by 58.56% at the expense of 3.33% increase in capital investment, whereas the variable speed column secures a 62.06% savings in operating cost (OC) against an increase of capital investment (CI) by 1.83%.

Furthermore, we compare the CO_2 emission levels in Table 6. The CRBD fueled by natural gas produces CO_2 of 66.53 ton/yr. On this basis, we estimate the reduction of about 46.75 and 51.23% emissions locally for the fixed speed and variable speed VRRBD column, respectively. As far as global emissions are concerned, around a 80.16 and 81.80% reduction has been achieved. We further compare the emission levels in case of low sulfur diesel fuel used in both the utility systems and the central power plant. It is evident from Table 6 that we get very close savings with those

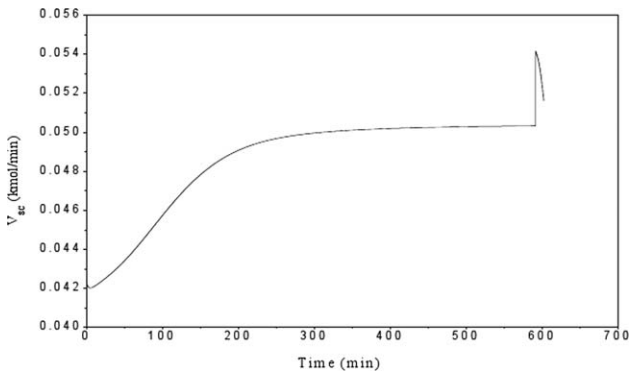

Figure 12. Manipulation profile of V_{8C} during the production phase of variable speed VRRBD.

Table 5. Comparison of Estimated Capital and Operating Costs under Open-Loop Operation

Cost Component	CRBD	Fixed Speed VRRBD	Variable Speed VRRBD
Hardware			
Column shell	30,494.92	30,494.92	30,494.92
Column tray	1672.97	1672.97	1672.97
Reboiler	28,622.39	28,622.39	28,622.39
Condenser	13,869.01	436.33	436.03
Compressor	–	15,921.76	14,802.85
Total CI	74,659.29	77,148.37	76,029.16
Utility			
Electricity	–	1988.53	1814.54
Cooling water	323.84	0.977	0.982
Steam	5244.37	317.64	296.96
Total OC	5568.21	2307.15	2112.48
TAC	30,454.64	28,023.27	27,455.53
TAC savings (%)	–	7.98	9.85

observed for natural gas in terms of both the total local emissions (TLE) and the total global emissions (TGE).

By analyzing the performance quantitatively, we observe that the variable speed VRRBD scheme shows better performance in terms of energy consumption, TAC and emissions over its fixed speed counterpart. Thus, we select the variable speed heat integrated column for closed-loop control study.

Closed-loop control algorithm

As stated earlier, the control objective is to recover the most volatile component (i.e., ethyl acetate) at a constant purity by adjusting the reflux rate. Additionally, the liquid holdup in reflux drum is to be controlled by the manipulation of distillate rate. To investigate the improvements achieved by the closed-loop variable speed VRRBD over its open-loop counterpart, the CRBD is continued as a reference process. Accordingly, the GSPI controller is designed for top product composition and the holdup in reflux drum is maintained by using a conventional PI controller. The control

Table 6. Comparative CO_2 Emissions under Open-loop Operation

	CO_2 Emissions (ton/yr)		
Terms	CRBD	Fixed Speed VRRBD	Variable Speed VRRBD
Natural gas (*fuel*)			
Emissions from steam boiler	66.53	4.03	3.77
Emissions from gas turbine	–	31.40	28.68
TLE	66.53	35.43	32.45
TLE savings (%)	–	46.75	51.23
Emissions saved at power station	–	−22.23	−20.34
TGE	66.53	13.20	12.11
TGE savings (%)	–	80.16	81.80
Low sulfur diesel (*fuel*)			
Emissions from steam boiler	93.45	5.66	5.23
Emissions from gas turbine	–	44.03	40.32
TLE	93.45	49.69	45.55
TLE savings (%)	–	46.83	51.26
Emissions saved at power station	–	−31.23	−28.57
TGE	93.45	18.46	16.98
TGE savings (%)	–	80.25	81.83

Table 7. Controller Specifications and Performance

Items	GSPI	Conventional PI
Gain (K_C/K_{C0})	3.7	−0.001
Time constant (τ_I), min	0.2	0.2
ISE (Figure 13)	1.1463×10^{-5}	7.4×10^{-3}

parameter values are documented in Table 7. It should be pointed out that both the controllers are switched on only in production phase.

Constant Composition Control. The setpoint composition has been fixed at a value of 0.964, which is originally the steady-state distillate composition. This value typically imposes a limit in the achievable product purity under batch operation. Figure 13 depicts the dynamics of the variable speed VRRBD column under the GSPI control law. This simulation experiment shows that the setpoint is maintained almost up to the end of the operation. Moreover, the GSPI controller responds against the error signal smoothly. Despite large distillate rate fixed as bias signal (68% of V_8 at steady state), the controller shows its ability in obtaining constant composition product.

Interestingly, by the end of the batch operation, the reflux rate should be increased very rapidly to keep the product on specification. Our results are in agreement with this physical interpretation. This typical characteristic indicates the considerable decrease of process gain by the end of the operation.

Table 8 summarizes the performance improvements achieved by the controlled VRRBD column. Compared to

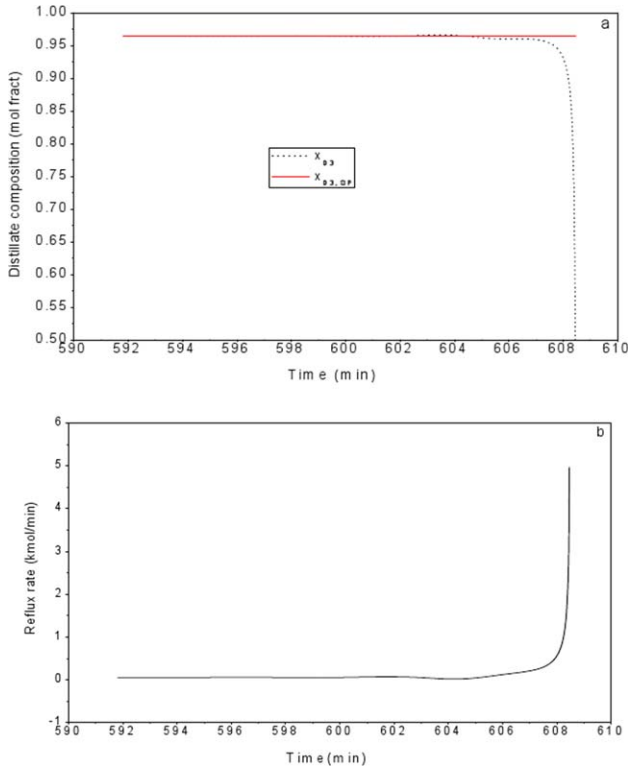

Figure 13. Dynamics of variable speed VRRBD column under GSPI controller: (a) constant composition control and (b) reflux rate profile.

[Color figure can be viewed in the online issue, which is available at wileyonlinelibrary.com.]

Table 8. Comparative Performance Improvements

Item	Open-Loop Variable Speed VRRBD	Closed-Loop Variable Speed VRRBD
Average product composition (mol fract)	0.9283	~0.964
Total distillate withdrawn (kmol)	0.3658	0.4631
Production period (min)	10.75	13.65

the open-loop process, the closed-loop VRRBD provides distillate product with a higher purity. Moreover, the closed-loop process produces relatively large amount of distillate. Actually, the product in closed-loop operation is enriched with mainly ethyl acetate (Figure 13), while relatively large quantity of ethanol (reactant) leaves the column (Figure 4) degrading the product quality during the production period of open-loop operation. This indicates a better forward reaction rate attained in the closed-loop column during the production phase, yielding more product quantity.

Quantitative Performance Analysis. Here, it is interesting to compare the variable speed VRRBD scheme under the GSPI controller with the CRBD column. It is inspected that the controlled process secures an energy savings of 82.62%. Simulation results concerning economic outcomes are summarized in Table 9, and we notice a TAC savings of 10.17%. As far as CO_2 emissions are concerned, around a 50.83 and 81.41% reduction in TLE and TGE, respectively, is achieved for natural gas (Table 10). In case of low sulfur diesel fuel, the corresponding savings are 51.01 and 81.58%. It should be highlighted that the closed-loop VRRBD offers the potential benefits as highlighted in Table 8 without compromising its thermodynamic efficiency and economic performance, and its ability to cut emissions.

Concluding Remarks and Future Work

In this article, a novel VRBD is proposed. An open-loop control policy is developed to ensure the optimal use of internal heat source, thereby leading to a simultaneous abatement of the OC, TAC, and greenhouse gas emissions. Performing several numerical simulations, it is observed that the VRRBD column appears overwhelmingly superior to its conventional counterpart. We further notice that the VRRBD in conjunction with a variable speed compressor shows a better performance compared to that with a fixed speed compressor.

Subsequently, we chose the variable speed VRRBD for synthesizing the GSPI controller aiming to produce ethyl acetate at a constant composition. For the example reactive system, we investigate that the closed-loop variable speed VRRBD meets the end objective of relatively high-purity product. Moreover, the closed-loop process produces more amount of distillate as compared to the open-loop VRRBD. It is worth noticing that the closed-loop variable speed VRRBD achieves these appealing advantages without compromising its energy efficiency performance, cost benefit, and its ability to cut emissions.

After being confirmed about the superiority of the proposed heat integrated scheme over the conventional column, it is suitable to further consider a dynamic optimization approach to minimize energy use or maximize product recovery by varying both the CR and the reboiler heat load. This issue is not treated in this article, but will be discussed elsewhere.

Table 9. Comparison of Estimated Capital (Main Equipment) and Operating (Utilities Per Year) Costs for the Closed-Loop CRBD and Variable Speed VRRBD Columns

Cost Component	Closed-Loop CRBD	Closed-Loop Variable Speed VRRBD
Hardware		
Column shell	30,494.92	30,494.92
Column tray	1672.97	1672.97
Reboiler	28,622.39	28,622.39
Condenser	14,198.01	436.03
Compressor	–	14,802.85
Total CI	74,988.29	76,029.16
Utility		
Electricity	–	1814.54
Cooling water	322.66	0.98
Steam	5244.37	296.96
Total OC	5567.03	2112.48
TAC	30,563.13	27,455.53
TAC savings (%)	–	10.17

Table 10. Comparative CO_2 Emissions Under Closed-Loop Operation

Terms	CO_2 Emissions (ton/yr)	
	Closed-Loop CRBD	Closed-Loop Variable Speed VRRBD
Natural gas (*fuel*)		
Emissions from steam boiler	66.53	3.98
Emissions from gas turbine	–	28.73
TLE	66.53[a]	32.71
TLE savings (%)	–	50.83
Emissions saved at power station	–	−20.34
TGE	66.53[a]	12.37
TGE savings (%)	–	81.41
Low sulfur diesel (fuel)		
Emissions from steam boiler	93.45	5.42
Emissions from gas turbine	–	40.36
TLE	93.45	45.78
TLE savings (%)	–	51.01
Emissions saved at power station	–	−28.57
TGE	93.45	17.21
TGE savings (%)	–	81.58

[a]It is same for both open-loop and closed-loop CRBD, because in both cases, the operating hours/year, external heat input to the still (i.e., Q_R) and temperature at which the steam is delivered are identical.

Literature Cited

1. U.S. National Academies Report, 2008. Available at: http://americasclimatechoices.org/climate_change_ 2008_final.pdf (accessed May 2009).
2. Houghton J. Global warming and climate change—a scientific update. *Environ Prot Bull* 2002;066:21–26.
3. Gadalla MA, Olujic Z, Jansens PJ, Jobson M, Smith R. Reducing CO_2 emissions and energy consumption of heat-integrated distillation systems. *Environ Sci Technol*. 2005;39:6860–6870.
4. EPA, Environmental Protection Agency, 1999. Available at: http://www.epa.gov/globalwarming/climate/ index.html (accessed August 2002).
5. DTI, Department of Trade and Industry, 2000. Available at: http://www.dti.gov.uk/epa/bpmar2001.pdf (accessed August 2002).
6. Salamon P, Nulton JD. The geometry of separation processes: a horse–carrot theorem for steady flow systems. *Europhys Lett*. 1998;42:571–576.
7. De Koeijer G, Kjelstrup S. Minimizing entropy production rate in binary tray distillation. *Int J Appl Thermodyn*. 2000;3:105–110.

8. Petlyuk FB, Platanov VM, Slavinskii DM. Thermodynamically optimal method for separating multicomponent mixtures. *Int Chem Eng*. 1965;5:555–561.
9. Dünnebier G, Pantelides CC. Optimal design of thermally coupled distillation columns. *Ind Eng Chem Res*. 1999;38:162–176.
10. Kolbe B, Wenzel S. Novel distillation concepts using one-shell columns. *Chem Eng Proc*. 2004;43:339–346.
11. Kaibel B, Jansen H, Zich E, Olujic Z. Unfixed dividing wall technology for packed and tray distillation columns. *Distillation Absorption*. 2006;152:252–266.
12. Kiss AA, Rewagad RR. Energy efficient control of a BTX dividing-wall column. *Comput Chem Eng*. 2011;35:2896–2904.
13. Liu X, Qian J. Modeling, control, and optimization of ideal internal thermally coupled distillation columns. *Chem Eng Technol*. 2000;23:235–241.
14. Naito K, Nakaiwa M, Huang K, Endo A, Aso K, Nakanishi T, Nakamura T, Noda H, Takamatsu T. Operation of a bench-scale ideal heat integrated distillation column (HIDiC): an experimental study. *Comput Chem Eng*. 2000;24:495–499.
15. Lee JY, Kim YH, Hwang KS. Application of a fully thermally coupled distillation column for fractionation process in naphtha reforming plant. *Chem Eng Process*. 2004;43:495–501.
16. Fukushima T, Kano M, Hasebe S. Dynamics and control of heat integrated distillation column (HIDiC). *J Chem Eng Jpn*. 2006;39:1096–1103.
17. Huang K, Shan L, Zhu Q, Qian J. Adding rectifying/stripping section type heat integration to a pressure-swing distillation (PSD) process. *Appl Therm Eng*. 2008;8:923–932.
18. Shenvi AA, Herron DM, Agrawal R. Energy efficiency limitations of the conventional heat integrated distillation column (HIDiC) configuration for binary distillation. *Ind Eng Chem Res*. 2011;50:119–130.
19. Suphanit B. Optimal heat distribution in the internally heat-integrated distillation column (HIDiC). *Energy*. 2011;36:4171–4181.
20. Fonyo Z, Kurrat R, Rippin DWT, Meszaros I. Comparative analysis of various heat pump schemes applied to C_4 splitters. *Comput Chem Eng*. 1995;19:S1–S6.
21. Henley EJ, Seader JD. Equilibrium-Stage Separation Operations in Chemical Engineering. New York: Wiley, 1981.
22. Diez E, Langston P, Ovejero G, Romero MD. Economic feasibility of heat pumps in distillation to reduce energy use. *Appl Therm Eng*. 2009;29:1216–1223.
23. Jogwar SS, Baldea M, Daoutidis P. Tight energy integration: dynamic impact and control advantages. *Comput Chem Eng*. 2010;34:1457–1466.
24. Jana AK, Mane A. Heat pump assisted reactive distillation: wide boiling mixture. *AIChE J*. 2011;57:3233–3237.
25. Schmal JP, Van Der Kooi HJ, De Rijke A, Olujić Z, Jansens PJ. Internal versus external heat integration: operational and economic analysis. *Chem Eng Res Des*. 2006;84:374–380.
26. Annakou O, Mizsey P. Rigorous investigation of heat pump assisted distillation. *Heat Recov Syst CHP*. 1995;15:241–247.
27. Takamatsu T, Tajiri A, Okawa K. In: Proceedings of the Chemical Engineering Conference of Japan, Nagoya, 1998, pp. 628–629.
28. Maiti D, Jana AK, Samanta AN. A novel heat integrated batch distillation scheme. *Appl Energy*. 2011;88:5221–5225.
29. Johri K, Babu GUB, Jana AK. Performance investigation of a variable speed vapor recompression reactive batch rectifier. *AIChE J*. 2011;57:3238–3242.
30. Babu GUB, Pal EK, Jana AK. An adaptive vapor recompression scheme for a ternary batch distillation with a side withdrawal. *Ind Eng Chem Res*. 2012;51:4990–4997.
31. Bahar A. Modeling and Control Studies for a Reactive Batch Distillation Column. Ph.D. Thesis, Chemical Engineering Department, Middle East Technical University, Ankara, 2007.
32. Freshwater DC. Thermal economy in distillation. *Chem Eng Res Des*. 1951;29A:149–160.
33. Douglas JM. Conceptual Design of Chemical Processes, 1st ed. New York: McGraw-Hill, 1988.
34. Iwakabe K, Nakaiwa M, Huang K, Nakanishi T, Røsjorde A, Ohmori T, Endo A, Yamamoto T. Energy saving in multicomponent separation using an internally heat-integrated distillation column (HIDiC). *Appl Therm Eng*. 2006;26:1362–1368.
35. Smith R, Delaby O. Targeting flue gas emissions. *Trans IChemE*. 1991;69:492–505.
36. Economic Indicator. *Chem Eng*. August 2011;2nd Quarter:56.
37. Suphanit B. Design of internally heat-integrated distillation column (HIDiC): uniform heat transfer area versus uniform heat distribution. *Energy*. 2010;35:1505–1514.
38. Jana AK, Radha Krishna Adari PV. Nonlinear state estimation and control of a batch reactive distillation column. *Chem Eng J*. 2009;150:516–526.
39. Bequette BW. Process Control: Modeling, Design, and Simulation. New Delhi: Prentice-Hall, 2003.
40. Mujtaba IM, Macchietto S. Efficient optimization of batch distillation with chemical reaction using polynomial curve fitting techniques. *Ind Eng Chem Res*. 1997;36:2287–2295.
41. Jana AK. Chemical Process Modelling and Computer Simulation, 2nd ed. New Delhi: Prentice-Hall, 2011.
42. Monroy-Loperena R, Alvarez-Ramirez J. Output-feedback control of reactive batch distillation columns. *Ind Eng Chem Res*. 2000;39:378–386.

Manuscript received Aug. 11, 2012, and revision received Jan. 19, 2013.